Biochemical and Biophysical Research Communications **256,** 13–19 (1999)
Article ID bbrc.1999.0279, available online at http://www.idealibrary.com on IDEAL®

# Transverse Elasticity of Myofibrils of Rabbit Skeletal Muscle Studied by Atomic Force Microscopy

Yoshihiro Yoshikawa,* Toshihiro Yasuike,* Akira Yagi,† and Takenori Yamada*,[1]

**Department of Physics (Biophysics Section), Faculty of Science, Science University of Tokyo, Shinjuku-ku, Tokyo 162-8601, Japan; and †Olympus Optical Co., Hachioji, Tokyo 192-0032, Japan*

Received January 25, 1999

**Surface structure of myofibrils of rabbit skeletal muscle and their transverse elasticity were studied by atomic force microscopy. Images of myofibrils had a periodic structure characteristic of sarcomeres of skeletal muscle fibers. The transverse elasticity distribution in the sarcomere was determined based on force-distance curves measured at various loci of single myofibrils. The Z-line in rigor myofibrils was the most rigid in all the loci of myofibrils studied under various physiological conditions. The overall transverse elasticity of myofibrils decreased in the order in rigor solution > +AMPPNP solution > relaxing solution. The "apparent" transverse Young's modulus of myofibrils estimated at the overlap region between thin and thick filaments was 84.0 ± 18.1, 37.5 ± 14.0, and 11.5 ± 3.5 kPa in rigor, +AMPPNP, and relaxing solution respectively.** 

Skeletal muscle fiber is composed of a bundle of myofibrils which have a characteristic striation of sarcomeres (1). The contractile force is produced by the interaction of cross-bridges extruded from thick filaments with thin filaments (2). The produced force is transferred to the both ends of fiber through a series of sarcomeres in which Z-line mechanically links the adjacent sarcomeres. Therefore the sarcomere is the contractile unit of skeletal muscle fiber, which produces force, transmits it along the fiber, and sustains the produced strains (3).

The longitudinal mechanical properties of muscle fibers has been studied by applying sudden or sinusoidal length changes to muscle fibers and analyzing the resulting force responses. Such studies indicated that the longitudinal elasticity of muscle fibers dominantly comes from the cross-bridges attached to thin filaments (4, 5) and the thin filaments (6, 7, 8). On the other hand, the transverse mechanical properties of muscle fibers have been studied by compressing fibers with osmotic pressure and analyzing the changes of the actomyosin filament spacing (9) and the fiber width (10, 11), or by measuring the propagation velocity of ultrasonic waves across muscle fiber (12).

The atomic force microscope (AFM) has recently been developed to obtain images of specimens based on ups and downs of their surface structure, in which a tip of cantilever was scanned over the specimens and its deflection at each locus was detected to produce computer-assisted images of the specimens (13). AFM can also be applied to study the elasticity of various biological materials (14, 15, 16, 17) based on the deflection of the cantilever produced by pressing its tip to specimens. In the present studies, we used this AFM technique to investigate the transverse elasticity of myofibrils of skeletal muscle fibers under various physiological conditions. Preliminary results have been reported (18).

## MATERIALS AND METHODS

*Preparation of single myofibrils.* Single myofibrils were prepared from glycerinated muscle fibers as described previously (19). Fiber bundles of the rabbit psoas muscle were skinned in a relaxing solution containing 1.0% Triton X-100 and stored in a 50% glycerol in relaxing solution at −20°C for 5-12 weeks before use. A short bundle of glycerinated fibers was cut into pieces with scissors, put in a relaxing solution, and homogenized with a Polytron homogenizer (PT1200; Kinematica, Switzerland), which produced a suspension of myofibrils containing single myofibrils. Myofibrils were prepared from glycerinated muscle fibers freshly before experiments.

*AFM observations of myofibrils.* Two types of AFM (NV2500 and NVB100; Olympus Optical Co., Tokyo, Japan) were used in the present studies, both of which were incorporated in an inverted optical microscope. These AFMs make it possible to observe an appropriate locus of specimens in solution by positioning the tip of the AFM cantilever under optical microscope. Commercially available cantilevers made of silicon nitride (micro cantilever PR400PB: Olympus Optical Co.) were used, which had the spring constant of 0.02 N/m and the tip radius of 30–50 nm.

[1] To whom correspondence should be addressed. Fax: +81-3-5261-1023. E-mail: yamada@rs.kagu.sut.ac.jp.

Abbreviations used: AFM, atomic force microscope; AMPPNP, adenyl-5′-yl-imidodiphosphate; EGTA, O,O′-bis(2-aminoethyl)ethyleneglycol-N,N,N′,N′-tetraacetic acid.



0006-291X/99 $30.00

Myofibrils were attached to glass substrate for AFM experiments. First, a fresh cover glass (18 × 18 mm; Matsunami, Osaka, Japan) was dipped in a saturated KOH solution for ca. 2 h. Then it was sonicated in distilled water with a sonicator (B-220H; Branson, Connecticut, USA) followed by a wash with ethanol. After the glass surface got dried, a drop of myofibril suspension was put on the cover glass thus treated. After standing it for ca. 5 min, the cover glass was gently washed with a flesh relaxing solution to remove unattached or weakly attached myofibrils. It was then pasted to the bottom of a plastic dish (type 1006; Falcon, New Jersey, USA) with the myofibril-attached side up. After filling the dish with a relaxing solution, it was set on the microscope stage of AFM. The solution in the dish was exchanged to an appropriate solution to change the physiological conditions of myofibrils.

By observing with the optical microscope, myofibril preparations firmly attached to the cover glass were selected and the cantilever tip was positioned at an appropriate locus of the preparations. (a) To obtain AFM images, the caltilever tip was approached to the preparation and scanned (usually by the tapping-mode) at a scan rate of 0.5-1 Hz with 256 data points. (b) To obtain force-distance curves as detailed below, the cantilever tip was approached to the preparation at a speed of 1 $\mu$m/s.

All experiments were made at room temperature (20-24°C).

*Measurements of the transverse elasticity of single myofibrils.* The transverse elasticity of myofibrils was studied based on the force-distance curve which can be obtained by use of a measurement mode equipped in the present AFMs. The force-distance curves represents the deflection of cantilever as a function of the distance between the cantilever tip and the surface of preparation. When a cantilever is approached to a preparation, its tip eventually attaches to the surface of the preparation. As the cantilever is further lowered, it presses the preparation and deflects upward; i.e., the more it deflects the more the preparation is rigid. The stiffness of the preparation is determined as the applied force divided by the indentation of the tip in the preparation. The force applied to the preparation can be calculated from the deflection of cantilever based on its spring constant while the indentation of the cantilever tip in the preparation is equal to the distance of cantilever lowered from the surface of preparation minus the deflection of cantilever.

It should be kept in mind that the radius of cantilever tips (30-50 nm) was only slightly greater than the spacing of myofilament lattices and Z-line networks exposed to the surface of myofibrils, 15-30 nm (20). Therefore the tip might indent in myofibrils not by producing a uniform dent but by breaking in preparations when it was pressed to the preparations. To prevent this from happening we used cantilevers with a blunt tip for force-distance measurements. Cantilevers with a blunt tip were selected from commercially purchased cantilevers based on force-distance curves against silicone rubbers; i.e., blunt tips produce relatively steep upward deflection. The cantilevers thus selected had the tip radius of ca. 50 nm under a scanning electron microscope (S2400; Hitachi, Tokyo).

*Chemicals.* ATP, and adenyl-5′-yl-imidodiphosphate (AMPPNP) respectively were purchased from Sigma Chemicals (St. Louis, USA) and Boehringer-Mannheim (Mannheim, Germany). O,O′-Bis(2-aminoethyl)ethyleneglycol-N,N,N′,N′-tetraacetic acid (EGTA) was purchased from Dojindo Laboratories (Kumamoto, Japan). All other chemicals were of analytical grade and purchased from Wako Chemicals (Osaka, Japan).

*Composition of solutions.* The composition of solutions was as follows (in mM); relaxing solution: $K^+$-propionate, 93; $MgCl_2$, 5; EGTA, 10; Imidazole, 20; ATP, 5; +AMPPNP solution: $K^+$-propionate, 121; $MgCl_2$, 5; $CaCl_2$, 2.3; EGTA, 2; Imidazole, 20; AMPPNP, 2.5; rigor solution: $K^+$-propionate, 109; $MgCl_2$, 5; EGTA, 10; Imidazole, 20. The pH of the solutions was adjusted to 7.0. The ionic strength was 160 mM.

## RESULTS

*AFM images of myofibrils.* A typical AFM image of a bundle of myofibrils in rigor solution is shown in Fig. 1(A). In Fig. 1(B) is shown a detailed image of the surface of a myofibril. As can be seen, single myofibrils were ca. 1 $\mu$m in diameter and had a characteristic sarcomere pattern with filamentous structures running along the surface of preparations. The distance between adjacent Z-lines was 2.0–2.2 $\mu$m. The width of A-band, I-band, Z-line, and M-region was ca. 1.6, 0.4-0.6, 0.13, and 0.17 $\mu$m respectively. If we take the radius of cantilever tip into consideration, these values reasonably agree with the geometry of sarcomere structure of rabbit skeletal muscle at slack length (see the references in (19)). It was generally noted that successive AFM images obtained at the same location of myofibrils became gradually deteriorated suggesting that the scanning of cantilever tip may damage the surface structure of myofibrils.

AFM images of myofibrils in +AMPPNP and relaxing solution showed similar periodic sarcomere structures, but, different from those of myofibrils in rigor solution, almost no filament structures could be observed in the images. As myofibrils in these solutions are much elastic compared with those in rigor solution to be described below, their surface structures might have been deformed during the scanning of cantilever tip.

*Transverse elasticity of single myofibrils.* To study the transverse elasticity of myofibrils, force-distance curves were measured at various loci of myofibrils. The cantilever tip can be positioned roughly at an appropriate locus by observing preparations under optical microscope or more precisely based on their AFM images. However as the surface of preparations may be damaged associated with previous cantilever scannings, we measured force-distance curves from unscanned loci of myofibril preparations. This was made as follows. As can be seen in Fig. 2(A), the myofibril preparations further extended from the segment where an AFM image was obtained. By extrapolating the sarcomere geometry in the AFM image as shown in Fig. 2(B), we positioned the cantilever tip at an appropriate locus in one or two unscanned sarcomeres neighboring to it (e.g., (1) to (4) in Fig. 2(B)). In the following only the very first force-distance curve measured at a locus was used for analysis.

In Fig. 3(A) are shown typical force-distance curves thus obtained at various loci of the sarcomere of myofibrils in rigor solution. It can be seen that the upward slope in the force-distance curves is less steep in the order of at the Z-line > the overlap region > the M-region ≥ the I-band. This indicates that the transverse elasticity of rigor myofibrils increases in the order at Z-line, the overlap region, the M-region, and the I-band

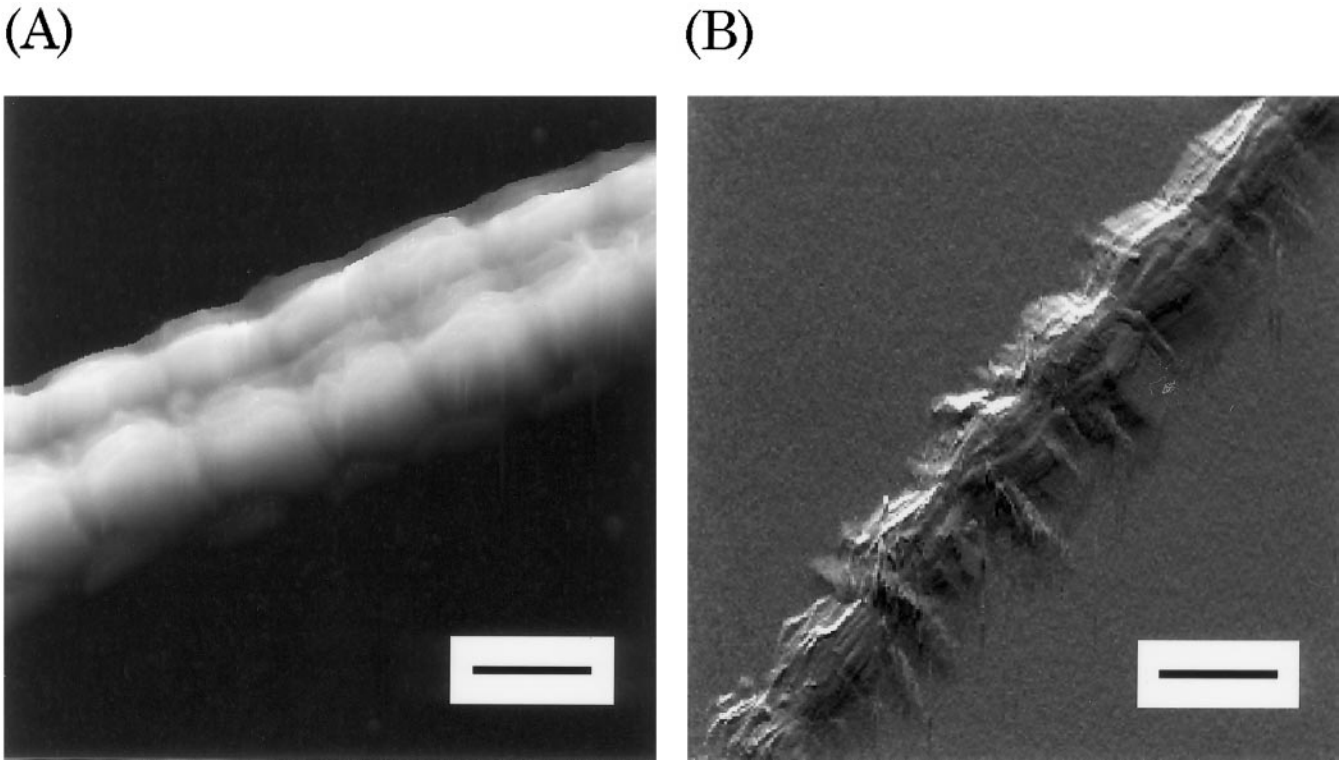


**FIG. 1.** (A) A typical AFM image of a bundle of myofibrils in rigor solution. Scale bar: 2 $\mu$m. (B) A detailed AFM image of the surface of a myofibril. Scale bar: 2 $\mu$m.

in which the elasticity of the last two loci were nearly the same.

In Fig. 3(B) are shown typical force-distance curves obtained at the overlap region between thin and thick filaments of myofibrils in various physiological solutions. The upward slope in the force-distance curves is

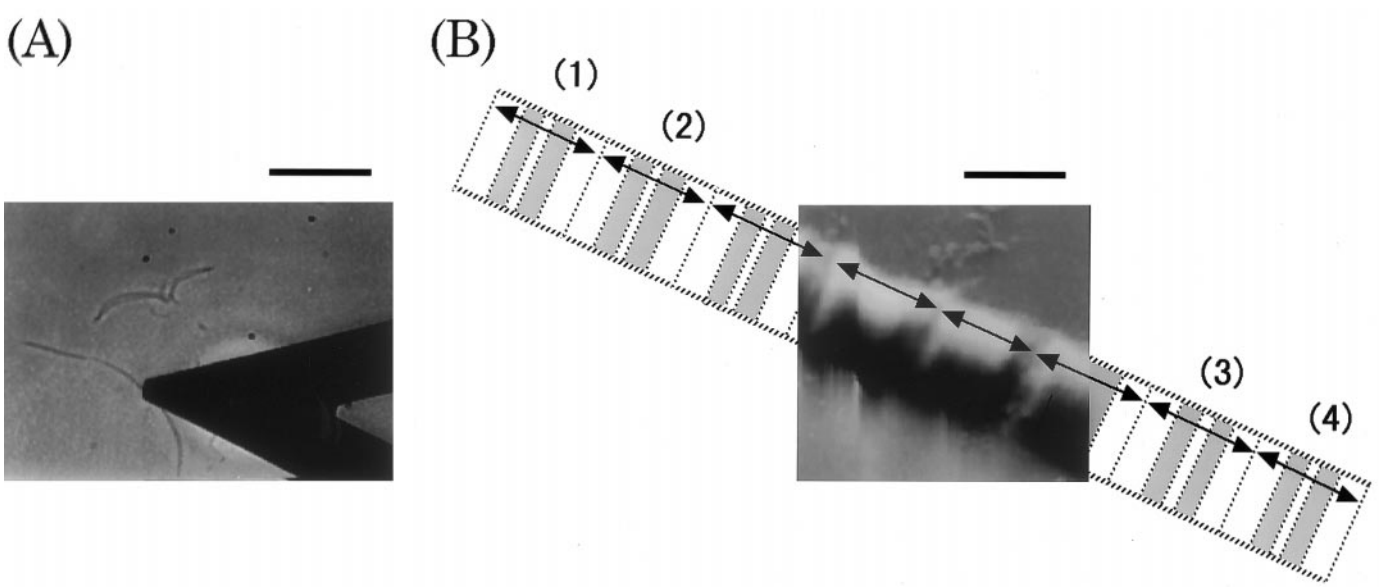


**FIG. 2.** (A) An optical microscope image of a cantilever positioned on a myofibril. Scale bar: 20 $\mu$m. (B) A schematic drawing showing how a specific locus of unscanned sarcomeres in a myofibril is determined. A central square shows an AFM image of a segment of the myofibril preparation (5 $\times$ 5 $\mu$m; scale bar, 2 $\mu$m). Each sarcomere is specified by a double-headed arrow. See the details in the text.

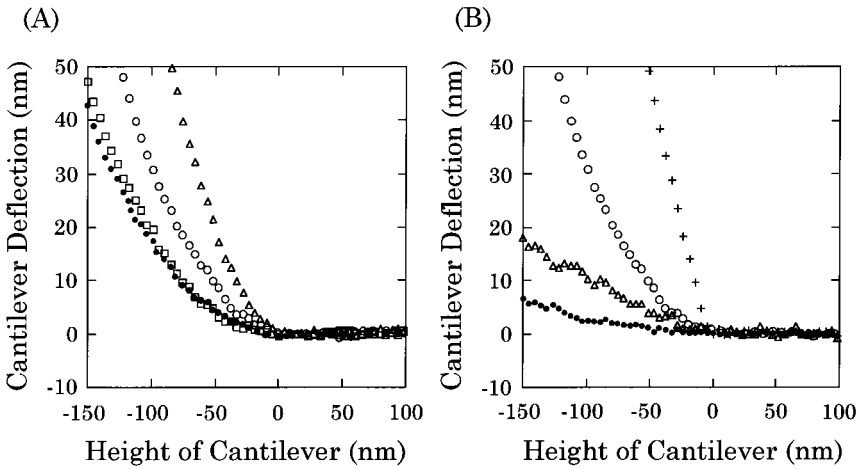


**FIG. 3.** (A) Typical force-distance curves obtained at various loci of single myofibrils in rigor solution. (△) Z-line, (○) the overlap region between thin and thick filaments, (□) M-region, and (●) I-band. (B) Typical force-distance curves obtained at the overlap region of single myofibrils in various physiological solutions. (○) Rigor solution, (△) +AMPPNP solution, and (●) relaxing solution. Included is a force-distance curve for cover glass (+). The origin of the cantilever height of each force-distance curve was determined as the position from which the cantilever started to deflect upward.

less steep in the order for myofibrils in rigor solution > those in +AMPPNP solution > those in relaxing solution, indicating that the elasticity of the overlap region increases in the order in rigor, +AMPPNP, and relaxing solution. In the same figure, a force-distance curve obtained for cover glass is included for comparison. It can be seen that the magnitude of the upward deflection of cantilever is equal to that of the downward shift of cantilever position indicating that the cantilever tip is pressed to non-elastic material.

Force-distance curves were similarly measured at 15 separate loci equally spaced from a Z-line to the next Z-line in each sarcomere of myofibrils in these solutions. In the upward slope in some of the force-distance curves obtained at I-band and M-region of myofibrils in rigor and +AMPPNP solution, however, sudden downward deflections of cantilever by 3-5 nm were observed when the cantilever indented in preparations by 50-100 nm. In the case of myofibrils in relaxing solution such anormal deflections of cantilever were never observed under comparable situations. As pointed out in Materials and Methods, these findings suggest that the cantilever tip may have broken in the filaments lattice of myofibrils associated with such abnormal deflections. Taking this artifacts into consideration, the stiffness of myofibrils was determined in the following as the force required to make the cantilever indent in myofibrils by 25 nm in rigor solution, by 45 nm in +AMPPNP solution and by 60 nm in relaxing solution respectively. The transverse stiffness of the sarcomere of myofibrils in various solutions thus obtained are summarized in Fig. 4.

It can be seen that (i) the overall stiffness of myofibrils decreases in the order in rigor, +AMPPNP, and relaxing solution, (ii) the Z-line of rigor myofibrils is the most rigid, (iii) in each solution, all the loci in the overlap region have nearly the same stiffness, and (iv)

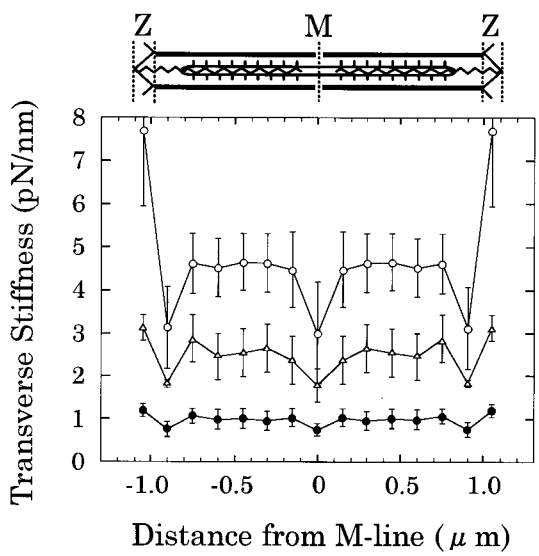


**FIG. 4.** Distribution of the transverse stiffness along the sarcomere of myofibrils in various physiological solutions. (○) Rigor solution, (△) +AMPPNP solution, and (●) relaxing solution. The data obtained at various loci of sarcomeres were analyzed by assuming that each half-sarcomere structure is the mirror-image to the M-line. Each data point is the averaged value from 20 to 30 separate experiments. The error bar represents the standard deviation. At the top is shown a schematic sarcomere structure having a sarcomere length of 2.1 $\mu$m, which is composed of thin filaments extending from Z-lines (Z), a thick filament connected to the Z-lines by zigzag filaments of connectins (or titins), and M-line (M) at the center. The axial scale of the sarcomere is adjusted to the horizontal scale of the lower figure. See the details in the text.

the stiffnesses of I-band and M-region are almost the same and are slightly smaller than that of the overlap region. Based on the (iii) above, all the stiffness data for the overlap region in each solution were averaged. Then the transverse stiffness at Z-line, I-band, the overlap region, and M-region of myofibrils was 7.7 ± 1.8 (mean ± S.D.) (n = 22), 3.3 ± 1.4 (n = 42), 4.6 ± 0.7 (n = 140), and 3.0 ± 1.2 (n = 14) pN/nm in rigor solution, 3.1 ± 0.3 (n = 6), 1.8 ± 0.2 (n = 4), 2.6 ± 0.5 (n = 120), and 1.8 ± 0.4 (n = 11) pN/nm in +AMPPNP solution, and 1.2 ± 0.2 (n = 11), 0.8 ± 0.2 (n = 13), 1.0 ± 0.2 (n = 95), and 0.7 ± 0.2 (n = 12) pN/nm in relaxing solution respectively.

## DISCUSSION

*Distribution of the transverse elasticity along myofibrils and its dependency on the physiological conditions.* Myofibrils prepared in the present study had a sarcomere length of 2.0-2.2 $\mu$m, indicating that the overlap between thin and thick filaments is maximal (19). As shown in Results, the transverse elasticity of myofibril substantially depended on the loci in sarcomeres as well as on the physiological conditions.

As can be seen in Fig. 4, the transverse stiffness at the overlap region of myofibrils decreased in the order in rigor solution > +AMPPNP solution > relaxing solution. In accord with this, Nyland et al. (17) reported based on similar AFM experiments that the transverse stiffness of myofibrils of insect flight muscle decreases in the order of in rigor, activation, and relaxation. Considering the dissociation constant for myosin head from thin filaments under comparable conditions (1), these results indicate that the transverse stiffness of myofibrils is greater as the affinity of myosin heads to thin filaments is greater. Thus we may conclude that the actomyosin filament lattice in sarcomere is stabilized in the transverse direction dominantly by the attachment of cross-bridges with thin filaments.

On the other hand, it has been reported that the velocity of ultrasonic wave (7 MHz) propagating across muscle fibers decreases when the fibers contract (12) indicating that the transverse stiffness decreases associated with contraction. As cross-bridges attach to thin filaments in contracting muscle fibers, this result could be explained as the ultrasonic waves propagate not through actomyosin filament lattice but through some other structures, for example the intracellular water of muscle fibers (21).

As can also be seen in Fig. 4, the Z-line in rigor myofibrils is the most rigid in all the loci of myofibrils studied in various solutions ($P < 0.005$). This is consistent with the role of Z-line as a mechanical wall of sarcomere structure. However it can also be noted that, compared with the Z-line of myofibrils in rigor solution, the Z-lines in +AMPPNP and relaxing solution are more elastic. This does not go with the general view that Z-line is composed of a zigzag network of $\alpha$-actinin (3) and its structural stability not affected by changing the bathing solution as above. This can be explained as follows. The Z-line network is connected to one ends of the thin filament array in its adjacent half sarcomeres. The other ends of the thin filaments interact with cross-bridges extruded from thick filaments in the overlap region. These assembly of the filament lattices mechanically supports the Z-line network. When Z-line is pressed by the cantilever tip, the Z-line may be compressed vertically and/or make a tilt. If Z-line tilts, thin filaments connected to it may be pulled and slipped out from the overlap region as the longitudinal stiffness of thin filaments is large enough (22). Therefore the magnitude of the tilting depends on how strongly the thin filaments attach to thick filaments in the overlap region. In myofibrils in rigor solution, the Z-line may be stably hold in the transverse direction as all the crossbridges attach to thin filaments (23). However, in myofibrils in +AMPPNP and relaxing solution, the affinity of crossbridges to thin filament is weak compared with those in rigor solution (1) so that the Z-line becomes relatively unstable in the transverse direction and may tilt accordingly. The tilting apparently increases the transverse elasticity of the Z-line. Therefore the greater transverse elasticity of Z-lines in myofibrils in +AMPPNP and relaxing solution may be artifacts due to tiltings of Z-line.

It can also be noted that I-band and M-line are similarly flexible and they are slightly more flexible than the overlap region in rigor myofibrils ($P < 0.005$). This is consistent with high flexural elasticities of thin filaments (24) and connectin (or titin) (25, 26) which are the major components of these loci. Further the transverse stiffness of I-band as well as M-line decreases in the order of myofibrils in rigor solution, in +AMPPNP solution, and in relaxing solution. As discussed above in the case of the transverse stiffness of Z-line, these could be explained as the slipppage between thin and thick filaments in the overlap region associated with the compression by cantilever.

*Estimation of the 'apparent' transverse Young's modulus of myofibrils.* In order to understand the structural stabilities of myofibrils at the molecular level, it will be helpful to express the elasticity of myofibrils in terms of the Young's modulus. To estimate the Young's modulus of specimens based on experiments as in the present studies, the Hertz formulas is generally used. It gives the relation between the applied force and the indentation of materials when a uniform sphere is pressed to a uniform rod (27). As the cantilever tip is much harder and its radius much smaller than those of myofibrils, the Hertz formulas can be simplified as

$$\delta = \lambda \sqrt[3]{\frac{9P^2}{64R}\left(\frac{1-\sigma^2}{E}\right)^2},$$

where δ represents the indentation of cantilever tip in myofibril; E, the transverse Young's modulus of myofibril; $\sigma$, the Poisson's ratio; λ, the Lame's constant; R, the radius of cantilever tip; P, the force applied to the cantilever. Parameters used were $\sigma = 0.5$ by assuming isovolumic changes; $\lambda = 2.1$ (as is given in (27)); $R = 50$ nm.

Although myofibrils are not uniform at the present molecular level (1), all the force-distance curves for myofibrils obtained in the present studies, except for those obtained at Z-lines of rigor myofibrils, were found to be fit successfully with the above Hertz equation up to 15-20 nm of the cantilever deflection (or up to 40 nm of indentation of myofibrils). We therefore estimated the 'apparent' transverse Young's modulus of myofibrils at the overlap region between thin and thick filaments based on the above equation. By the least mean square method, we calculated a value for the Young's modulus which makes the above equation best fit to the data in the above mentioned ranges of each force-distance curve. The "apparent" transverse Young's modulus of myofibrils thus estimated was 84.0 ± 18.1 kPa (n = 20) in rigor solution, 37.5 ± 14.0 kPa (n = 16) in +AMPPNP solution, and 11.5 ± 3.5 kPa (n = 11) in relaxing solution respectively. Greater values for the corresponding transverse Young's modulus of myofibrils obtained in our preliminary study (18) were found to be due to errors in the calculations.

Let us briefly consider the molecular situation in myofibrils when force-distance curves were measured. When the cantilever tip is lowered to the overlap region of myofibrils, it firstly pushes thin and thick filaments at the surface of myofibrils producing strains to underlying cross-bridges which anchor the thin and thick filament. In the present experiments, the cantilever pressed the surface of myofibrils with the force of up to ca. 0.3-0.4 nN (assuming the deflection of ca. 15-20 nm and the spring constant of 0.02 N/m). As the force to break a rigor complex is known to be ca. 10 pN (28), a significant amount of attached cross-bridges near the surface of rigor myofibrils could be ruptured due to the compression by the cantilever tip. In the case of myofibrils in +AMPPNP and relaxing solution, further more cross-bridges attached to thin filaments may be ruptured as the actomyosin interactions are much weaker in these solutions. These may significantly decrease the stiffness. Thus the intrinsic transverse stiffness of actomyosin lattice in myofibrils could be somewhat greater than the above values.

In any case the magnitudes of the transverse Young's modulus obtained above were comparable to those determined from changes of the fiber diameter by osmotically compressing skinned muscle fibers; i.e. the radial stiffness for rigor and relaxed fibers was 17-39 and 15-16 kPa respectively (10, 11). On the other hand, the magnitude of the longitudinal Young's modulus for single muscle fibers has been reported as ca. 30 MPa for rigor glycerinated rabbit muscle fibers (29) and ca. 36 kPa for relaxed skinned frog muscle fibers (30). Therefore the transverse Young's modulus of muscle fibers may be significantly smaller than the longitudinal Young's modulus under comparable conditions indicating that the actomyosin filament lattice in sarcomere is more rigid along the fiber axis than perpendicular to it.

The magnitude of the Young's modulus for myofibrils as above may be compared to those of 5% gelatin (20 kPa) (14), platelets (1-50 kPa) (15), and cardiocytes (10-200 kPa) (16).

## ACKNOWLEDGMENTS

We are grateful to Dr. T. Ando, Kanazawa University, for his kind advice on the AFM measurements. We also appreciate T. Hayashi and E. Imai, Olympus Optical Co., for their technical supports. This work was supported in part by Grant-in-Aids for Scientific Research (B-07458175 and C-09680658) from the Ministry of Education, Science, Sports and Culture of Japan (to T.Y.).

## REFERENCES

1. Bagshaw, C. R. (1993) *Muscle Contraction*, Chapman & Hall, London, UK.
2. Huxley, H. E. (1969) The mechanism of muscular contraction. *Science* **164,** 1356–1366.
3. Squire, J. M. (1997) Architecture and function in the muscle sarcomere. *Curr. Opin. Struct. Biol.* **7,** 247–257.
4. Ford, L. E., Huxley, A. F., and Simmons, R. M. (1981) The relation between stiffness and filament overlap in stimulated frog muscle fibres. *J. Physiol. (Lond.)* **311,** 219–249.
5. Julian, F. J., and Sollins, M. R. (1975) Variation of muscle stiffness with force at increasing speeds of shortening. *J. Gen. Physiol.* **66,** 287–302.
6. Huxley, H. E., Stewart, A., Sosa, H., and Irving, T. C. (1994) X-ray diffraction measurements of the extensibility of actin and myosin filaments in contracting muscle. *Biophys. J.* **67,** 2411–2421.
7. Wakabayashi, K., Sugimoto, Y., Tanaka, H., Ueno, Y., Takezawa, Y., and Amemiya, Y. (1994) X-ray diffraction evidence for the extensibility of actin and myosin filaments during muscle contraction. *Biophys. J.* **67,** 2422–2435.
8. Higuchi, H., Yanagida, T., and Goldman, Y. E. (1995) Compliance of thin filaments in skinned fibers of rabbit skeletal muscle. *Biophys. J.* **69,** 1000–1010.
9. Matsubara, I., Goldman, Y. E., and Simmons, R. M. (1984) Changes in the lateral filament spacing of skinned muscle fibres when cross-bridges attach. *J. Mol. Biol.* **173,** 15–33.
10. Maughan, D., and Godt, R. (1981) Radial forces within muscle fibers in rigor. *J. Gen. Physiol.* **77,** 49–64.
11. Umazume, Y., and Kasuga, N. (1984) Radial stiffness of frog skinned muscle fibers in relaxed and rigor conditions. *Biophys. J.* **45,** 783–788.
12. Tamura, Y., Hatta, I., Matsuda, T., Sugi, H., and Tsuchiya, T. (1982) Changes in muscle stiffness during contraction recorded using ultrasonic waves. *Nature* **299,** 631–633.

13. Binning, G., Quate, C. F., and Gerber, C. (1986) Atomic Force Microscopy. *Phys. Rev. Lett.* **56,** 930–933.
14. Radmacher, M., Fritz, M., and Hansma, P. K. (1995) Imaging soft samples with the atomic force microscope: gelatin in water and propanol. *Biophys. J.* **69,** 264–270.
15. Radmacher, M., Fritz, M., Kacher, C. M., Cleveland, J. P., and Hansma, P. K. (1996) Measuring the viscoelastic properties of human platelets with the atomic force microscope. *Biophys. J.* **70,** 556–567.
16. Hofmann, U. G., Rotsch, C., Parak, W. J., and Radmacher, M. (1997) Investigating the cytoskeleton of chicken cardiocytes with the atomic force microscope. *J. Struct. Biol.* **119,** 84–91.
17. Nyland, L., Petersen, J., and Maughan, D. (1997) Functional and morphometric study of *Drosophila* indirect flight muscle using atomic force microscopy. *Biophys. J.* **72,** A102.
18. Yasuike, T., Yoshikawa, Y., and Yamada, T. (1998) AFM studies of surface structures of myofibrils of rabbit skeletal muscle. *J. Muscle Res. Cell Motil.* **19,** 446.
19. Yuri, K., Wakayama, J., and Yamada, T. (1998) Isometric contractile properties of single myofibrils of rabbit skeletal muscle. *J. Biochem.* **124,** 565–571.
20. Squire, J. (1981) *The Structural Basis of Muscular Contraction.* Plenum Press, New York.
21. Yamada, T. (1998) $^{1}$H-Nuclear magnetic resonance evidence for acto-myosin-dependent structural changes of the intracellular water of frog skeletal muscle. *Biochim. Biophys. Acta* **1379,** 224–232.
22. Kojima, H., Ishijima, A., and Yanagida, T. (1994) Direct measurement of stiffness of single actin filaments with and without tropomyosin by *in vitro* nanomanipulation. *Proc. Natl. Acad. Sci.* **91,** 12962–12966.
23. Cooke, R., and Franks, K. (1980) All myosin heads form bonds with actin in rabbit rigor skeletal muscle. *Biochemistry* **19,** 2265–2269.
24. Yanagida, T., Nakase, M., Nishiyama, K., and Oosawa, F. (1984) Direct observation of motion of single F-actin filaments in the presence of myosin. *Nature* **307,** 58–60.
25. Maruyama, K., Matsubara, S., Natori, R., Nonomura, Y., Kimura, S., Ohashi, K., Murakami, F., Honda, S., and Eguchi, G. (1977) Connectin, an elastic protein of muscle. Characterization and function. *J. Biochem.* **82,** 317–337.
26. Wang, K., Ramirez-Mitchell, R., and Palter, D. (1984) Titin is an extraordinary long, flexible and slender myofibrillar protein. *Proc. Natl. Acad. Sci. (USA)* **81,** 3685–3689.
27. Roark, R. J. (1965) *Formulas for Stress and Strain.* McGraw-Hill, New York.
28. Nishizaka, T., Miyata, H., Yoshikawa, H., Ishiwata, S., and Kinosita, K., Jr. (1995) Unbinding force of a single motor molecule of muscle measured using optical tweezers. *Nature* **377,** 251–254.
29. Tawada, K., and Kimura, M. (1984) Stiffness of glycerinated rabbit psoas fibers in the rigor state. *Biophys. J.* **45,** 593–602.
30. Maughan, D. W., and Godt, R. E. (1979) Stretch and radial compression studies on relaxed skinned muscle fibers of the frog. *Biophys. J.* **28,** 391–402.